PPPL--2488

DE88 009349

X-ray Transitions in Highly Charged Neonlike Ions

P. Beiersdorfer, S. von Goeler, M. Bitter, E. Hinnov, R. Bell, S. Bernabei, J. Felt, K. W. Hill, R. Hulse, J. Stevens, S. Suckewer, J. Timberlake, and A. Wouter

Princeton University, Plasma Physics Laboratory, Princeton, New Jersey 08544, USA

M. H. Chen, J. H. Scofield, D. D. Dietrich, M. Gerassimenko, E. Silver, and R. S. Walling

University of California, Lawrence Livermore National Laboratory, Livermore, California 94550, USA

P. L. Hagelstein

Massachussettes Institute of Technology, Research of Laboratory Electronics, Cambridge, MA 02139

Abstract

Wavelength measurements of n=3 to n=2 transitions in neonlike Xe^{44+}, La^{47+}, Nd^{50+}, and Eu^{53+} have been made using a high-resolution Bragg-crystal spectrometer on the Princeton Large Torus tokamak. The measurements cover the wavelength regions 2.00—3.00 Å and include the electric dipole, and the electric and magnetic quadrupole transitions. The measured wavelengths are compared to energy levels obtained from a multiconfigurational Dirac-Fock calculation. Systematic differences between the experimental and theoretical values are found, which vary smoothly with atomic number. The magnitude of the differences depends on the particular type of transition and ranges from -2.8 eV to +2.2 eV. Inclusion of electron correlation corrections due to ground state correlations and (super) Coster-Kronig type fluctuations in the theoretical energies is shown to reduce the differences for some but not all types of transitions.

I. Introduction

The spectra of very highly charged ions can provide detailed information on the structure of multi-electron systems in a strong Coulomb field. Therefore, high-resolution wavelength measurements of spectral lines emitted from few-electron, high-Z systems can be used to check the accuracy of multiconfigurational relativistic atomic structure calculations.

Systematic comparisons between experimental and theoretical transition energies have been made recently by Seely *et al.* for $4p \rightarrow 4s$ transitions in copperlike ions and for $3d \rightarrow 3p$ transitions in cobaltlike ions for elements up to uranium.[1] In the case of the cobaltlike transitions the comparison between experimental observations and theoretical values from Dirac-Fock calculations showed a discrepancy of about 3 eV. This discrepancy has since been removed by including electron correlation corrections to the theoretical transition energies.[2]

High-resolution data on $\Delta n = 1$ x-ray transitions in multi-electron systems such as the $3 \rightarrow 2$ x-ray transitions in neonlike systems have been obtained only recently, and the existing data show some disagreement with theoretical wavelengths. A high-resolution measurement of the $3 \rightarrow 2$ transitions in neonlike silver has been made on the Princeton Large Torus (PLT).[3] The measurements showed systematic discrepancies between observed and calculated wavelengths which depended on the type of transition. It was found that the experimental wavelengths of the $3p, 3s \rightarrow 2p$ transitions were shorter than the values predicted by a relativistic atomic structure calculation.[3] The experimental wavelengths of the $3d \rightarrow 2p$ transitions were determined to be slightly longer, and those of the $3p \rightarrow 2s$ transitions considerably longer than the predicted values.[3] Similar discrepancies between experimental and theoretical wavelengths of the $3p \rightarrow 2s$ transitions were inferred from observations of the x-ray transitions in neonlike bismuth in beam-foil experiments.[4] The authors speculated that this discrepancy may be due to inadequacies in the calculation of quantum electrodynamical corrections, in particular of the self-energy. However, the experimental uncertainties of about 6 eV were too large to obtain a definite result. The small amount of high-resolution data obtained

to date has so far been insufficient to perform a detailed comparison of theory and experiment as a function of atomic number Z .

In this paper we extend the high-resolution measurements of the 3 → 2 transitions in neonlike silver (Z=47) made previously[3] to the rare earth elements. In particular, we report on measurements of the $\Delta n=1$ electric dipole, electric quadrupole, and magnetic quadrupole transitions of neonlike xenon (Z=54), lanthanum (Z=57), neodymium (Z=60), and europium (Z=63), which fall into the x-ray region between 2.00 2.19 and 2.29 3.00 A. The spectra were observed on PLT from discharges with high electron temperatures of up to 6.5 keV using a high-resolution Bragg-crystal spectrometer. The uncertainty in the wavelength measurements is ±0.1 mA for most transitions and corresponds to a relative error of $\Delta\lambda/\lambda \approx 1:20000$.

The data presented in this paper have allowed us to make detailed comparisons between the experimental results and theoretical values which have been obtained from a multiconfigurational Dirac-Fock (MCDF) code developed by Grant and co-workers,[5,6] and which include QED corrections. Although the agreement is generally excellent, small, yet significant differences have been found, which, as in the case of silver,[3] depend on the type of transition. The magnitude of the differences ranges from about +2.2 eV for transitions of the type $3p, 3s \cdot 2p$ to as much as -2.8 eV for transitions of the type $3d, 3p \rightarrow 2s$. In order to understand these discrepancies, we have also made a simple estimate of the residual electron correlation energy arising from electron ground state correlations and from (super) Coster-Kronig type fluctuations. We find that including the estimate for the residual electron correlation energy in the theoretical transition energies reduces the differences between theoretical and experimental wavelengths for many transitions. However, the residual electron correlation energy cannot account for all differences, and considerable discrepancies remain for some types of transitions.

II. - Experimental Arrangement

The n=3 to n=2 transitions in Xe^{44+}, La^{47-}, Nd^{50+}, and Eu^{53-} were measured using the PLT high-resolution Bragg-crystal spectrometer in Johann

geometry.[7] The spectrometer employs a 11-in$\times 3\frac{3}{4}$-in$\times$0.06-in silicon crystal cut to the 220 plane with a $2d_{\infty}$-spacing of 3.8400 Å and bent to a radius of curvature of 365 cm. Most measurements were performed with the illuminated length of the crystal varying between 2.5 cm and 10 cm. In the region below 2.19 Å an illuminated length of about 18 cm was used, in order to maintain an adequate count rate during the measurements of europium. The detector is oriented perpendicular to the line connecting the crystal and the center of the detector, and not tangent to the Rowland circle, as described in Refs. 3 and 7. As a result, the best focus is achieved in the center of the detector, and the resolution decreases toward the edges. In the wavelength range of interest, 2.00—3.00 Å, the resolution of the central part of the spectrum varied from $\lambda/\Delta\lambda \approx 1200$ to $\lambda/\Delta\lambda \approx 8000$. For comparison, the Doppler-broadened line width of xenon corresponded to $\lambda/\Delta\lambda \approx 5000$ at ion temperatures of 1 keV which were typical for the plasma conditions. Six settings were necessary to span the wavelength regions 2.00—2.19 and 2.29—3.00 Å. No measurements were taken in the region between 2.19 and 2.29 Å due to insufficient machine time.

The minimum central electron temperature necessary to observe $3 \rightarrow 2$ transitions of a given neonlike ion with our instrument on PLT is shown in Fig. 1. The maximum central electron temperature achieved in PLT was approximately 6.5 keV as determined by Thomson scattering. This temperature enabled us to observe the transitions between the $(2p^5_{3/2}3s_{1/2})_{J=1,2}$ upper states and the ground state in Eu^{53+}, although the signal was faint. The line-averaged electron density in these discharges was 1.0×10^{13} cm^{-3}. The high electron temperatures were obtained with a modest amount of lower-hybrid, radio-frequency heating power $P_{LH} \approx 650$ kW using a side-launching, 16-grill waveguide.[8,9]

At each electron temperature shown in Fig. 1 a certain fractional abundance of the corresponding neonlike ions is reached in the center of the plasma. For instance, according to coronal equilibrium values of Breton *et al.*,[10] the electron temperature of 3.8 keV corresponds to a fractional abundance of about 8% of xenon in the neonlike state, Xe^{44+}. Similar neonlike ion fractions are predicted by coronal equilibrium calculations for silver, neodymium, and eu-

ropium. Coronal equilibrium calculations, however, overestimate the actual abundance in a tokamak plasma. A more realistic equilibrium calculation which includes plasma transport and charge-exchange recombination with neutral hydrogen predicts lower fractions of neonlike ions in PLT plasmas.[11]

Lanthanum, neodymium, and europium were injected into PLT plasmas via laser blow-off.[12] Xenon was puffed into the plasma using a fast gas valve. In addition, argon and scandium have been introduced into the plasma in order to use the resulting hydrogenlike resonance lines as wavelength references. Furthermore, titanium, chromium, manganese, and a small amount of vanadium were indigenous to the plasma, and the hydrogen- and heliumlike spectra of these elements have also been recorded.

III. Experimental Results

An overview of the spectral range investigated is given in Fig. 2 which shows the location of the main $\Delta n=1$ neonlike lines as well as the location of the various hydrogen- and heliumlike spectra which were observed. We have normalized our measurements to the theoretical values for the hydrogenic transitions given in Refs. 13, 14, and 15, since these wavelengths can be calculated with the highest accuracy.[13-16] In doing so we find that the measured wavelengths of the heliumlike resonance lines $1snp\ ^1P_1 \rightarrow 1s^2\ ^1S_0$ of scandium, titanium, vanadium, and chromium are consistently between 0.1 and 0.2 mÅ shorter than predicted by Vainshtein and Safronova.[17] A similar discrepancy between measured and calculated values for the heliumlike resonance lines had been reported earlier[3] and may indicate that the theoretical wavelengths computed by Vainshtein and Safronova[17] are somewhat too long.

The experimental values of the wavelengths of the $3s, 3p, 3d \rightarrow 2p$ and $3d, 3p \rightarrow 2s$ transitions are listed in Table I. They have been determined with respect to the theoretical wavelength values of the hydrogenic lines given in Table II. The procedures used to identify the neonlike transitions and to determine their respective wavelengths are similar to those described in Ref. 3 for the measurement of Ag^{37+}. The error in the wavelengths of the strong neonlike lines is predominantly determined by the dispersion of the spectrometer, as

discussed in Ref. 3. The error of weak lines is larger due to larger statistical errors at low count rates. A few transitions have been observed in different settings of the spectrometer. The wavelengths obtained with different settings were reproducible to within 0.1 mA.

Typical spectral data are shown in Figs. 3 and 4 for the case of neodymium. The spectrum in Fig. 3 contains transitions of the type $3s_{1/2} \rightarrow 2p_{3/2}$. The neonlike doublet $(2p^5_{3/2}3s_{1/2})_{J=1,2} \rightarrow 2p^6$, denoted $3G$ and $M2$, is readily identifiable. In addition, an array of sodium-, magnesium-, and possibly aluminum-like satellites can be seen on the long-wavelength side of these lines. The ratio of the satellite line intensity to the intensity of the neonlike lines in this case is considerably larger than the ratio observed previously in the spectrum of silver,[3] and may indicate a greater abundance of ions in the lower charge states. The spectrum of the electric dipole transition $3s_{1/2} \rightarrow 2p_{1/2}$, labelled $3F$, and of the electric dipole transition $3d_{5/2} \rightarrow 2p_{3/2}$, labelled $3D$, is shown in Fig. 4. Again strong satellites due to the corresponding transitions in ions in lower ionization states are seen in the spectrum. Since the detector is not tangent to the Rowland circle, but instead is oriented perpendicular to the line connecting the crystal and the center of the detector, the spectral regions observed with the edges of the detector have lower resolution than those observed with the the central part of the detector. This effect is especially strong in Fig. 4, where the width of line $3D$ is much larger than the width of line $3F$.

Subtraction of background spectra, as described earlier in Ref. 3, was required in only a few cases. The most notable case is due to a coincidence of line $3G$ in lanthanum with the resonance transition $1s2p\ ^1P_1 \rightarrow 1s^2\ ^1S_0$ in Ti^{20+}. As a result, the uncertainty of the measured wavelength of this line is larger than that of most other electric dipole lines.

All but one of the strong electric dipole transitions in neonlike xenon have been measured previously by Conturie *et al.* from laser-irradiated, imploding microballoons,[18] and several of the strong electric dipole transitions in lanthanum and neodymium have been measured by Aglitskii *et al.* in vacuum spark discharges.[19] The results of these measurements are listed in Table I for comparison. In all cases our values disagree with these prior measurements by several milliangstroms. This disagreement is larger than the errors quoted in

Refs. 18 and 19. Part of the disagreement could be due to the fact that theses authors used different transitions and correspondingly different theoretical wavelength values for the calibration of their wavelength measurements. The disagreement may also reflect a possible contamination of the neonlike lines by transitions in lower charge states as a result of the high density and transient nature of laser-produced or spark plasmas.

We have observed two electric quadrupole ($E2$) transitions of the type $3d_{5/2} \rightarrow 2s_{1/2}$, labelled $E2S$. Identification of this type of transition has been reported recently by Gauthier *et al.* in laser-produced plasmas for strontium, molybdenum, rhodium, and silver.[20] Further, we have observed $E2$ transitions of the type $3p \rightarrow 2p$. The longest-wavelength $E2$ line, denoted $E2L$ ("lower"), is relatively intense and thus can easily be identified in the spectrum. The shorter-wavelength $E2$ lines, denoted $E2M$ ("middle") and $E2U$ ("upper"), are the weakest features observed in the present spectra. Both have been identified in the case of xenon; only one of the two has been identified in lanthanum. The shortest wavelength $E2$ line in xenon, line $E2U$, partially blends with a line which may be due to a transition in a lower charge state, such as aluminum- or siliconlike xenon. Consequently, the value listed for this line in Table I is less certain than those of the other electric quadrupole lines in xenon. The electric quadrupole lines of neodymium which fall into the wavelength region monitored in the present experiment coincide with transitions in the $K\alpha$-spectra of heliumlike chromium and manganese. The $E2$ transitions in neodymium could not be identified even if background subtraction techniques were used.

Together with the electric dipole transitions of the type $3s \rightarrow 2p$ the electric quadrupole lines can be used to determine the energies of Δn=0 transitions within the n=3 shell. These transitions, in particular the transitions $(2p^5_{1/2}3p_{3/2})_{J=2} \rightarrow (2p^5_{1/2}3s_{1/2})_{J=1}$ and $(2p^5_{3/2}3p_{3/2})_{J=2} \rightarrow (2p^5_{3/2}3s_{1/2})_{J=1}$, are of interest in collisionally pumped soft x-ray laser schemes.[21,22] Several of the $3 \rightarrow 3$ intrashell transitions are listed in Table III. A direct measurement of the $3 \rightarrow 3$ transitions is very difficult due to the presence of many lines of nearly identical wavelength which have much higher intensity and which result from Δn=0 transitions in sodium-, magnesium-, and aluminumlike charge states.

The values in Table III indicate that the lasing wavelength in a collisionally pumped laser could be reduced to about 58.3 Å, if gain were achieved in a lanthanum target, compared to approximately 100 Å in silver,[3] and 200 Å in selenium.[21]

In the case of xenon we can compare our $\Delta n=0$ results to those obtained by Dietrich *et al.* in beam-foil measurements.[23] Table III shows that our values differ from those in Ref. 23 by amounts which are larger than quoted errors for the two $\Delta n=0$ transitions of the type $3d \rightarrow 3p$. Our values agree with those in Ref. 23 for the remaining three transitions of the type $3p \rightarrow 3s$.

Finally, we have also identified one n=4 to n=2 transition in neonlike xenon, which is listed in Table I and is denoted by $4D$. This transition is the $\Delta n=2$ analogue of transition $3D$.

IV. Theoretical Results and Comparison with Experiment

The energy levels of neonlike silver, xenon, lanthanum, neodymium, and europium have been calculated using the multiconfigurational Dirac-Fock code developed by Grant and co-workers.[5,6] The code offers several different choices of calculations, notably an optimal level (OL) calculation and an extended average level (EAL) calculation. In the OL calculation the basis state wavefunctions are optimized for a particular energy level; in the EAL calculation the wave functions are obtained by minimizing the average energy of all levels weighted by their respective statistical weights. The code takes into account the interaction between any two atomic electrons due to the exchange of a transverse photon through the use of the frequency-dependent Breit operator.[24] Further, it explicitly calculates corrections arising from QED effects.[6] In particular, the vacuum polarization is evaluated in second order according to a prescription given by Fullerton and Rinker.[25] The self-energy correction is calculated based on an effective charge approach.[6] This approach determines an effective nuclear charge for each orbital and interpolates among the hydrogenic self-energies tabulated by Mohr for the $1s_{1/2}, 2s_{1/2}, 2p_{1/2}$, and $2p_{3/2}$ levels.[26-28] For levels with principal quantum number $n \geq 3$ the n^{-3} scaling

rule[29] is used to estimate the self-energies.[6] In order to get the self-energy correction to a given transition energy, the sum of the self-energies of every electron in both the initial and final states is calculated and then subtracted. As a result, the procedure takes into account energy shifts due to relaxation effects. Effects due to the finite nuclear size are taken into account by employing the Fermi model for the nuclear charge distribution.[30]

The results of the MCDF calculations are listed in Table IV. All energies except those of the $3d \rightarrow 2p$ transitions labelled $3C'$ and $3D$ were obtained using the EAL procedure and including all 36 singly excited states with a hole in the $n = 2$ shell and a single electron in the $n = 3$ shell. The transition energy of line $4D$ in xenon was calculated in similar fashion by applying the EAL procedure to the $n = 4$ spectroscopic complex. For comparison we have calculated the transition energies of lanthanum using the OL approach. The resulting energies differ from the values obtained in the EAL calculation by less than 0.2 eV. The only exceptions are transitions $3C$ and $3D$. The theoretical energies obtained from the OL calculations are 0.7 eV lower in the case of transition $3C$ and 0.5 eV lower in the case of transition $3D$ than the values obtained from the EAL calculation. Consequently, we have recalculated the $3d \rightarrow 2p$ transition energies for all elements in the OL approach, since we deem the OL calculations to be more accurate. The resulting values are listed in Table IV. The relativistic Coulomb energies, $E_{Coulomb}$, the Breit interaction energies, E_{Breit}, and the QED corrections, which make up the total transition energy, E_{TOTAL}, are listed separately in Table IV. The calculations show that the QED corrections are a significant part of E_{TOTAL}. The QED corrections are largest for the transitions involving a $2s$-hole state, namely for the transitions labelled $3A$, $3B$, and $E2S$. In the case of lanthanum the calculated QED corrections of these levels is over 6 eV, which is about one part in one thousand. The predicted size of the radiative corrections of the $3s$ levels is considerably smaller. It ranges between 0.7 eV in silver to 1.8 eV in europium for the transitions $3G$ and $M2$, and is about 30% larger for transition $3F$.

In the last column of Table IV, a comparison is made between the theoretical energies and the experimental values. Here ΔE is defined as the difference

between the experimental minus the theoretical energy, i.e.,

$$\Delta E \equiv E_{exp} - E_{TOTAL}.$$

The uncertainty in ΔE is listed in the table and reflects solely the uncertainty in the experimental values. For this purpose the measured wavelengths given in Table I were converted to energies using the conversion constant hc/e = 12398.54 eVÅ.[31] We have included the values of ΔE for silver which we had measured earlier.[3] For consistency with the data for the higher-Z elements, the experimental energies of the silver transitions were re-referenced to hydrogenic calibration lines instead of the heliumlike reference lines used in Ref. 3. The re-referencing has had the effect of increasing the value of E_{exp} by approximately 0.3 eV.

The largest deviation of the theoretical energies from the experimental values is less than 2.8 eV, or 0.5 parts per thousand. A close examination of the differences shows that the differences are not random. Instead, ΔE exhibits systematic variations which depend on the type of transition, and which to a lesser extent also depend on Z. These variations can be seen in Fig. 5, where the values of ΔE are plotted separately for different types of transitions as a function of Z. The figure shows that ΔE is generally positive for transitions into a $2p$-vacancy state, and negative for transitions into a $2s$-vacancy state. The values of ΔE of the $3s \rightarrow 2p$ transitions, labelled $3G$ and $M2$, are plotted in Fig. 5(a). The values vary between 1.2 eV and 1.8 eV. Figure 5(a) also shows the values of ΔE of the $3d, 3p \rightarrow 2s$ transitions. In this case the average values decrease from about -1.4 eV in silver to -2.5 eV in lanthanum. The values of ΔE for the $3s \rightarrow 2p$ transitions, labelled $3F$, are shown in Fig. 5(b) and nearly equal those of $3G$ and $M2$ except for the point at Z = 60. The values of ΔE of the $3d \rightarrow 2p$ transitions are plotted in Fig. 5(c). For transitions $3D$, ΔE equals about +0.6 eV except in the case of xenon where ΔE vanishes. For the transitions $3C$, which involve states of different angular momentum, ΔE is slightly above +1 eV. In Fig. 5(d) we plot ΔE for transitions of the type $3p \rightarrow 2p$. The magnitude of ΔE is found to be about 0.5 eV larger for the $2p^5_{J=1/2}$-vacancy states than for the $2p^5_{J=3/2}$-vacancy states, although the values of ΔE for both types of transitions are comparable to the

values found for the $3s \rightarrow 2p$ transitions. The value of ΔE for transition $4D$ is also comparable to those of the $3s \rightarrow 2p$ transitions.

The EAL scheme used to calculate the values in Table IV includes configuration interaction from the same complex only. The same holds true for the OL scheme used to calculate the energies of the transitions $3C$ and $3D$. Consequently, we do not expect the theoretical transition energies given in Table IV to agree exactly with the experimental values. Instead we expect $\Delta E \approx E_C$, where E_C is the residual electron correlation energy. In the following we estimate the magnitude of E_C and compare its value to ΔE.

Ideally, the correlation contribution to the transition energy should be determined by calculating the total correlation energies of the ground state and each excited state and by taking the difference. However, since such a procedure is extremely involved, the simpler approach of Chen *et al.* is used.[2,32] Here the correlation energies of the passive electrons from the ground and excited state are assumed to cancel. The two dominant correlation corrections which remain after the cancellation are the ground state correlation correction, E_{gs}, and, in the case of the $2s$-hole states, the energy shift, E_{CK}, due to Coster-Kronig and super-Coster-Kronig fluctuations. Hence, $E_C \approx E_{gs}$ for the $2p$-hole states; and $E_C \approx E_{gs}+E_{CK}$ for the $2s$-hole states.

The ground state correlation energy arises because pairs are broken in the excitation. Since all pair energies are negative and since there are more pairs in the ground state than in the excited state, this effect increases the transition energies. As a result E_{gs} is positive. Furthermore, we make use of the findings by Öksüz and Sinanoğlu[33,34] that all-external pair correlation energies are approximately constant as a function of Z and as a function of the number of electrons in a given element. This allows us to estimate the residual pair correlation energy based on a nonrelativistic calculation of the pair energies for neutral zinc performed by Jankowski *et al.*[35] As a result we obtain $E_{gs} = 1.7$ eV for transitions involving a $2p$-vacancy state, and $E_{gs} = 1.0$ eV for transitions involving a $2s$-vacancy state.

The energies of the transitions $3d, 3p \rightarrow 2s$ are affected not only by ground state correlations but also by (super) Coster-Kronig fluctuations of the hole state.[2,32,36,37] This dynamic relaxation process in which the core hole fluctu-

ates to intermediate levels of the Coster-Kronig or super-Coster-Kronig type, reduces the transition energies. The effect can be accounted for by allowing for configuration interactions with the states $(2s^2 2p^4 3l3d)_{J=1,2}$ in the MCDF calculation and by using the OL method. The results of these calculations are given in Table V. The energy shift E_{CK} due to the (super) Coster-Kronig type fluctuations is obtained by subtracting E_{TOTAL} given in Table IV from E_{TOTAL} given in Table V. In the case of the $3p \rightarrow 2s$ electric dipole transitions the (super) Coster-Kronig fluctuations reduce the transition energies by 1.9 eV. The reduction is not as large for the energies of the $3d \rightarrow 2s$ electric quadrupole transitions. In this case the reduction is 0.9 eV.

The values of the residual electron correlation energy can now be obtained by adding the values for E_{gs} and E_{CK}. As a result we obtain $E_C \approx +1.7$ eV for all transitions into a $2p$-vacancy state, $E_C \approx -0.9$ eV in the case of the electric dipole transitions $3p \rightarrow 2s$, and $E_C \approx +0.1$ eV in the case for the electric quadrupole transitions $3d \rightarrow 2s$.

Comparing the values of E_C to those of ΔE we find that for many, but not all transitions the agreement of the theoretical energies with the experimental data is improved. E_C and ΔE are of comparable size, in particular for the transitions $M2$, $3G$, $3F$, $4D$, and $E2U$. Thus, the addition of E_C to E_{TOTAL} improves the agreement between theory and experiment in this case. The opposite is true for transitions $3D$ where the inclusion of E_C in the theoretical values worsens the agreement between theory and data. Addition of E_C to E_{TOTAL} reduces the discrepancy between theory and data for the transitions $3p \rightarrow 2s$. The remaining discrepancies for transition 3A range from as little as -0.74 eV in silver to -1.19 eV in xenon, and -1.36 eV in lanthanum. No improvement is achieved for the $3d \rightarrow 2s$ electric quadrupole transitions. The disagreement of the theoretical values with the data remains largest for these transitions and ranges from -2.55 eV in xenon to -2.88 eV in lanthanum.

Part of the discrepancy between the theoretical and experimental values may be due to inadequacies in treating the electron pair correlation energies. Our simple estimate is based on the nonrelativistic calculation for neutral zinc,[35] because no suitable relativistic calculation exists. A fully relativistic calculation of the correlation energies for high-Z neonlike systems could im-

prove our estimate considerably.

A further cause for the discrepancy between theoretical and experimental values may be an inadequate treatment of the self-energy contribution to the transition energy. Table IV shows that the radiative corrections are largest for the $2s$-vacancy states. Consequently, an error in the value of the self-energy will affect these levels the most, and, conversely, if there are problems with the radiative corrections, they will most likely be found in these levels. The values of the self-energy listed in Table IV are obtained from hydrogenic values which are adjusted for screening.[6] On the other hand, the use of hydrogenic self-energies[28] lowers the theoretical energies of the $3d, 3p \rightarrow 2s$ transitions by approximately 1.1 eV, 1.7 eV, and 2.0 eV in the case of silver, xenon, and lanthanum, respectively and improves the agreement with the data. The improved agreement, however, may be completely fortuitous. There is no *a priori* reason to believe that the use of hydrogenic self-energies (bare or screened) is valid in a regime where the orbitals are very much nonhydrogenic, as in the case of ten-electron, neonlike systems.

V. Summary

The emphasis of this paper has been to present a coherent set of wavelength data which can be used for comparison with theoretical results. In particular, we have reported on wavelength measurements of x-ray transitions in Xe^{44+}, La^{47+}, Nd^{50+}, and Eu^{53+} which were observed in the wavelength region 2.00—2.19 and 2.29—3.00 Å. The measurements include the strong electric dipole transitions $3d \rightarrow 2p$, $3s \rightarrow 2p$, and $3p \rightarrow 2s$ as well as the weaker electric quadrupole transitions $3p \rightarrow 2p$ and $3d \rightarrow 2s$. Further, the strong magnetic quadrupole transition $(2p_{3/2}^5 3s_{1/2})_{J=2} \rightarrow$ *ground state* has been observed for each element. We have also identified one $\Delta n=2$ transition of the type $4d \rightarrow 2p$ in neonlike xenon. The wavelength of each transition was determined with high accuracy (± 0.1 mÅ for most lines) with the help of a multitude of reference spectra from hydrogenlike ions.

Together with the wavelengths of neonlike silver measured earlier[3] the data have been used for comparison with multiconfigurational relativistic atomic

structure calculations. The comparisons reveal differences the magnitudes of which depend on the particular type of transition and which vary smoothly with Z. For all transitions to $2p$-vacancy states except transition $3D$ the magnitude ranges between +0.9 and +2.2 eV. For transition $3D$ the magnitude of the differences ranges only between zero and +0.6 eV. The residual electron correlation energy for the transitions into a $2p$-vacancy state has been estimated to equal $E_C \approx +1.7$ eV so that E_C is comparable in size to the magnitude of most differences. Consequently, adding E_C to the calculated energies improves the agreement of the theoretical values with the data for many transitions, especially in the case of the $3s \rightarrow 2p$ transitions. For the transitions into a $2s$-vacancy state the experimental energies are significantly less than those predicted by the MCDF calculations. Inclusion of electron correlations due to ground state correlations and (super) Coster-Kronig type fluctuations in the theoretical transition energies reduces the discrepancy between experimental and theoretical energies in the case of the $3p \rightarrow 2s$ transitions. The magnitude of the remaining discrepancies for transition $3A$ ranges from -0.76 eV in silver to -1.36 eV in lanthanum. Inclusion of residual electron correlations in the MCDF values does not diminish the discrepancy of the $3d \rightarrow 2s$ electric quadrupole transitions. Here the discrepancies are -2.55 eV and -2.88 eV in xenon and lanthanum, respectively. The discrepancies found after accounting for the additional electron correlations indicate strongly that further work is needed to resolve the differences.

The measurements presented in this paper were obtained in plasmas with electron temperatures in the range 4—6.5 keV. Based on the trends shown in Fig. 1 we can estimate that a peak electron temperature near 10 keV is needed to observe x-ray transitions in neonlike ions with atomic number Z≈70. Temperatures in this range may be achieved in tokamaks with additional electron heating power or with electron heating as a by-product of ion heating in fusion devices. High-resolution measurements of neonlike transitions in such very high-electron temperature plasmas are bound to yield new insights into our understanding of the structure of high-Z, multi-electron systems.

Acknowledgments

We are grateful for the support and encouragement provided by M. Eckart, H. Furth, A. Toor, and L. Wood. We would like to thank K. Mann, J. Anastasio, H. Anderson, and J. Gething, as well as J. Gorman, J. Lehner, and M. Saracino for their technical support. This work was supported by Lawrence Livermore National Laboratory under subcontracts No. SANL-622-033 and 8-668-705, and by the U. S. Department of Energy under contracts No. DE-AC02-76-CHO-3073 and W-7405-ENG-48. One of the authors (PB) was supported by the Fannie and John Hertz Foundation.

References

[1]J. F. Seely, J. O. Ekberg, C. M. Brown, U. Feldman, W. E. Behring, J. Reader, and M. C. Richardson, Phys. Rev. Lett. **57**, 2924 (1986).

[2]M. H. Chen , Phys. Rev. A **36**, 665 (1987).

[3]P. Beiersdorfer, M. Bitter, S. von Goeler, S. Cohen, K. W. Hill, J. Timberlake, R. S. Walling, M. H. Chen, P. L. Hagelstein, and J. H. Scofield, Phys. Rev. A **34**, 1297 (1986).

[4]D. D. Dietrich, G. A. Chandler, P. O. Egan, K. P. Ziock, P. H. Mokler, S. Reusch, and D. H. H. Hoffmann, Nucl. Instr. Meth. **B24/25**, 301 (1987).

[5]I. P. Grant, B. J. McKenzie, P. H. Norrington, D. F. Mayers, and N. C. Pyper, Comput. Phys. Commun. **21**, 207 (1980).

[6]B. J. McKenzie, I. P. Grant, and P. H. Norrington, Comput. Phys. Commun. **21**, 233 (1980).

[7]K. W. Hill, S. von Goeler, M. Bitter, L. Campbell, R. D. Cowan, B. Fraenkel, A. Greenberger, R. Horton, J. Hovey, W. Roney, N. R. Sauthoff, and W. Stodiek, Phys. Rev. A **19**, 1770 (1979).

[8]J. E. Stevens, R. Bell, S. Bernabei, A. Cavallo, T. K. Chu, P. Colestock, W. Hooke, J. Hosea, F. Jobes, T. Luce, E. Mazzucato, R. Motley, R. Pinsker, S. von Goeler, and J. R. Wilson, Nucl. Fus. (to be published).

[9]R. E. Bell, S. Bernabei, A. Cavallo, T. K. Chu, T. Luce, R. Motley, M. Ono, J. Stevens, and S. von Goeler, *Princeton Plasma Physics Laboratory* Report No. PPPL-2452, 1987.

[10]C. Breton, C. De Michelis, M. Finkenthal, and M. Mattioli, Fontenay-aux-Roses Laboratory Report No. EUR-CEA-FC-948, 1978.

[11]R. A. Hulse, Nucl. Tech. Fus. **3**, *259 (1983).*

[12]E. S. Marmar, J. L. Cecchi, and S. A. Cohen, Rev. Sci. Instrum. **46**, 1149 (1975).

[13]J. D. Garcia and J. E. Mack, J. Opt. Soc. Am. **55**, 654 (1965).

[14]G. W. Erickson, J. Phys. Chem. Ref. Data **6**, 831 (1977).

[15]W. R. Johnson and G. Soff, At. Data Nucl. Data Tables **33**, 405 (1985).

[16]P. Mohr, At. Data Nucl. Data Tables **29**, 453 (1983).

[17]L. A. Vainshtein and U. I. Safronova, Phys. Scripta **31**, 519 (1985).

[18]Y. Conturie, B. Yaakobi, U. Feldman, G. A. Doschek, R. D. Cowan, J. Opt. Soc. Am. **71**, 1309 (1981).

[19]E. V. Aglitskii, P. S. Antsiferov, A. M. Panin, and S. A. Ulitin, Opt. Spectrosc. (USSR) **60**, 122 (1986).

[20]J.-C.Gauthier, J.-P.Geindre, P. Monier, E. Luc-koenig, and J. Wyart, J. Phys. B: At. Mol. Phys. **19**, L385 (1986).

[21]D. L. Matthews, P. L. Hagelstein, M. D. Rosen, M. J. Eckart, N. M. Ceglio, A. U. Hazi, H. Medecki, B. J. Macgowan, J. E. Trebes, B. L. Whitten, E. M. Campbell, C. W. Hatcher, A. M. Hawryluk, R. L. Kauffman, L. D. Pleasance, G. Rambach, J. H. Scofield, G. Stone, and T. A. Weaver, Phys. Rev. Lett. **54**, 110 (1985).

[22]M. D. Rosen, P. L. Hagelstein, D. L. Matthews, E. M. Campbell, A. U. Hazi, B. L. Whitten, B. MacGowan, R. E. Turner, R. W. Lee, G. Charatis, G. E. Busch, C. L. Shepard, and P. D. Rockett, Phys. Rev. Lett. **54**, 106 (1985).

[23]D. D. Dietrich, G. A. Chandler, R. J. Fortner, C. J. Hailey, and R. E. Stewart, Phys. Rev. Lett. **54**, 1008 (1985).

[24]I. P. Grant and B. J. McKenzie, J. Phys. B **13**, 2671 (1980).

[25]L. W. Fullerton and G. A. Rinker, Jr., Phys. Rev. A **13**, 1283 (1976).

[26]P. J. Mohr, Ann. Phys. **88**, 52 (1974).

[27]P. J. Mohr, Phys. Rev. Lett. **34**, 1050 (1975).

[28]P. J. Mohr, Phys. Rev. A **26**, 2338 (1982).

[29]H. A. Bethe, Phys. Rev. **72**, 339 (1947).

[30]M. H. Chen, B. Crasemann, M. Aoyagi, K.-N. Huang, and H. Mark, At. Data Nucl. Data Tables **26**, 561 (1981).

[31]Value based on a 1984 revision of the Physical Constants by B. N. Taylor, in *X-Ray Data Booklet*, edited by D. Vaughan (Center for X-Ray Optics, Lawrence Berkeley Laboratory, University of California, Berkeley, 1986); E. R. Cohen and B. N. Taylor, J. Chem. Ref. Data **2**, 663 (1973).

[32]M. H. Chen, B. Crasemann, N. Mårtensson, and B. Johansson, Phys. Rev. A **31**, 556 (1985).

[33]İ. Öksüz and O. Sinanoğlu, Phys. Rev. **181**, 42 (1969).

[34]İ. Öksüz and O. Sinanoğlu, Phys. Rev. **181**, 54 (1969).

[35]K. Jankowski, P. Malinowski, and M. Polasik, J. Chem. Phys. **76**, 448 (1982).

[36]M. Ohno and G. Wendin, J. Phys. B **11**, 1557 (1978).

[37]M. Ohno and G. Wendin, J. Phys. B **12**, 1305 (1979).

Tables

TABLE I. Experimental wavelengths of the x-ray transitions observed in Xe^{44+}, La^{47+}, Nd^{50+}, and Eu^{53+}. Each wavelength is determined with respect to the wavelength of the hydrogenic reference line listed in the last column. The experimental uncertainties are indicated in parentheses, e.g., 2.4601(1) means 2.4601 ± 0.0001.

Element	*Upper Level*	*Key*	λ^{a}_{exp} (Å)	λ_{exp} (Å)	*Reference Line*
Xenon	$(2p^5_{3/2}3s_{1/2})_{J=2}$	$M2$	2.9449(1)		Ar Ly- δ
	$(2p^5_{3/2}3s_{1/2})_{J=1}$	$3G$	2.9411(1)	2.940[b]	Ar Ly δ
	$(2p^5_{3/2}3p_{1/2})_{J=2}$	$E2L$	2.8799(1)		Ar Ly ϵ
	$(2p^5_{3/2}3p_{3/2})_{J=2}$	$E2M$	2.8186(1)		Ar Ly $-\epsilon$
	$(2p^5_{1/2}3s_{1/2})_{J=1}$	$3F$	2.7288(1)	2.725[b]	Sc Ly $-\alpha_1$
	$(2p^5_{3/2}3d_{5/2})_{J=1}$	$3D$	2.7203(1)	2.718[b]	Sc Ly $-\alpha_1$
	$(2p^5_{1/2}3p_{3/2})_{J=2}$	$E2U$	2.6221(2.5)		Ti Ly $-\alpha_1$
	$(2p^5_{1/2}3d_{3/2})_{J=1}$	$3C$	2.5525(1)	2.549[b]	Ti Ly $-\alpha_1$
	$(2s_{1/2}3p_{1/2})_{J=1}$	$3B$	2.5052(1.5)		Ti Ly $-\alpha_1$
	$(2s_{1/2}3p_{3/2})_{J=1}$	$3A$	2.4601(1)		Ti Ly $-\alpha_1$
	$(2s_{1/2}3d_{5/2})_{J=2}$	$E2S$	2.3941(1)		Sc Ly $-\beta_1$
	$(2p^5_{3/2}4d_{5/2})_{J=1}$	$4D$	2.0957(1)		Cr Ly $-\alpha_1$
Lanthanum	$(2p^5_{3/2}3s_{1/2})_{J=2}$	$M2$	2.6133(1)		Ti Ly $-\alpha_1$
	$(2p^5_{3/2}3s_{1/2})_{J=1}$	$3G$	2.6100(2)	2.6142[c]	Ti Ly $-\alpha_1$
	$(2p^5_{3/2}3p_{1/2})_{J=2}$	$E2L$	2.5580(1)		Ti Ly $-\alpha_1$
	$(2p^5_{2/2}3d_{5/2})_{J=1}$	$3D$	2.4139(1)	2.4149[c]	Sc Ly $-\beta_1$
	$(2p^5_{1/2}3s_{1/2})_{J=1}$	$3F$	2.3965(1)		Sc Ly $-\beta_1$
	$(2p^5_{1/2}3p_{3/2})_{J=2}$	$E2U$	2.3019(2)		Sc Ly $-\beta_1$
	$(2s_{1/2}3p_{3/2})_{J=1}$	$3A$	2.1671(1.5)	2.1687[c]	Cr Ly $-\alpha_1$
	$(2s_{1/2}3d_{5/2})_{J=2}$	$E2S$	2.1108(1.5)		Cr Ly $-\alpha_1$
Neodymium	$(2p^5_{3/2}3s_{1/2})_{J=2}$	$M2$	2.3359(1)		Sc Ly $-\beta_1$
	$(2p^5_{3/2}3s_{1/2})_{J=1}$	$3G$	2.3331(1)		Sc Ly $-\beta_1$
	$(2p^5_{3/2}3d_{5/2})_{J=1}$	$3D$	2.1543(1.5)	2.1573[c]	Cr Ly $-\alpha_1$
	$(2p^5_{1/2}3s_{1/2})_{J=1}$	$3F$	2.1206(1.5)		Cr Ly $-\alpha_1$
Europium	$(2p^5_{3/2}3s_{1/2})_{J=2}$	$M2$	2.1015(2)		Sc Ly $-\beta_1$
	$(2p^5_{3/2}3s_{1/2})_{J=1}$	$3G$	2.0990(2)		Cr Ly $-\alpha_1$

[a] Present measurement.
[b] Conturie *et al.*, Ref. 18
[c] Aglitskii *et al.*, Ref. 19

TABLE II. Wavelengths of the hydrogenic transitions used as references in the measurement of the neonlike transitions. <> denotes average.

Reference Line	*Transition*	λ_{theory} (Å)
Ar $Ly-\delta$	$5P_{3/2} \rightarrow 1S_{1/2}, 5P_{1/2} \rightarrow 1S_{1/2}$	$< 2.91756 >^a$
Ar $Ly-\epsilon$	$6P_{3/2} \rightarrow 1S_{1/2}, 6P_{1/2} \rightarrow 1S_{1/2}$	$< 2.88095 >^a$
Sc $Ly-\alpha_1$	$2P_{3/2} \rightarrow 1S_{1/2}$	2.73602^b
Ti $Ly-\alpha_1$	$2P_{3/2} \rightarrow 1S_{1/2}$	2.49120^b
Sc $Ly-\beta_1$	$3P_{3/2} \rightarrow 1S_{1/2}$	2.31066^c
Cr $Ly-\alpha_1$	$2P_{3/2} \rightarrow 1S_{1/2}$	2.09014^b

[a]Garcia and Mack, Ref. 13
[b]Johnson and Soff, Ref. 15
[c]Erickson, Ref. 14

TABLE III. Experimental intrashell intervals in Xe^{44+} and La^{47+}.

Element	*Transition*	*Energy*[a] (*eV*)	*Energy*[b] (*eV*)
Xenon	$(2p^5_{3/2}3p_{1/2})_{J=2} \rightarrow (2p^5_{3/2}3s_{1/2})_{J=1}$	89.6 ± 0.4	89.1 ± 0.5
	$(2p^5_{3/2}3p_{3/2})_{J=2} \rightarrow (2p^5_{3/2}3s_{1/2})_{J=1}$	183.2 ± 0.4	182.9 ± 0.5
	$(2p^5_{1/2}3p_{3/2})_{J=2} \rightarrow (2p^5_{1/2}3s_{1/2})_{J=1}$	184.9 ± 0.7	186.5 ± 1
	$(2p^5_{3/2}3d_{5/2})_{J=1} \rightarrow (2p^5_{3/2}3p_{3/2})_{J=2}$	159.0 ± 0.3	157.2 ± 0.5
	$(2p^5_{1/2}3d_{3/2})_{J=1} \rightarrow (2p^5_{1/2}3p_{3/2})_{J=2}$	129.0 ± 0.7	131.3 ± 1
Lanthanum	$(2p^5_{3/2}3p_{1/2})_{J=2} \rightarrow (2p^5_{3/2}3s_{1/2})_{J=1}$	96.7 ± 0.4	
	$(2p^5_{1/2}3p_{3/2})_{J=2} \rightarrow (2p^5_{1/2}3s_{1/2})_{J=1}$	212.8 ± 0.4	

[a]Present measurement
[b]Dietrich *et al.*, Ref. 23

TABLE IV. Comparison between theoretical and experimental energies. The theoretical values were obtained from an extended average level calculation except transitions $3C$ and $3D$ which were calculated in the optimum level approach. $E_{Coulomb}$ is the relativistic Coulomb energy, E_{Breit} is the transverse Breit correction, E_{VP} is the vacuum polarization energy, E_{SE} is the self-energy, and E_{TOTAL} is the sum of the preceding columns. ΔE is defined as the difference between the experimental energies and E_{TOTAL}. The experimental values for xenon, lanthanum, neodymium, and europium are from Table I. The experimental values of silver are from Ref. 3. The uncertainties in ΔE are indicated in parentheses and are solely due to uncertainties in the experimental values; here 1.56(10) means 1.56 ± 0.10.

Element	*Key*	$E_{Coulomb}$ (eV)	E_{Breit} (eV)	E_{VP} (eV)	E_{SE} (eV)	E_{TOTAL} (eV)	ΔE (eV)
Silver	$M2$	3083.18	−4.39	−0.14	−0.83	3079.49	+1.56(10)
	$3G$	3087.72	−4.30	−0.14	−0.83	3084.12	+1.43(10)
	$E2L$	3161.95	−3.62	−0.02	−0.09	3158.23	+0.92(10)
	$E2M$	3213.26	−4.12	−0.02	−0.02	3209.11	+1.03(10)
	$3F$	3267.89	−7.29	−0.12	−1.11	3261.59	+1.25(10)
	$3D$	3339.82	−5.21	−0.02	−0.07	3334.53	+0.60(10)
	$E2U$	3392.42	−7.33	−0.00	−0.27	3385.36	+1.56(20)
	$3C$	3502.82	−7.95	−0.00	−0.19	3495.07	+1.05(10)
	$3B$	3605.64	−2.98	+0.44	−3.52	3599.59	−1.12(25)
	$3A$	3654.93	−3.73	+0.45	−3.47	3648.18	−1.64(10)
Xenon	$M2$	4214.66	−6.88	−0.26	+1.36	4208.88	+1.32(20)
	$3G$	4220.07	−6.74	−0.26	+1.36	4214.44	+1.17(20)
	$E2L$	4310.17	−5.61	−0.04	−0.23	4304.29	+0.98(20)
	$E2M$	4404.55	−6.49	−0.03	−0.11	4397.93	+0.87(30)
	$3F$	4552.50	−11.29	−0.18	+1.39	4542.42	+1.12(20)
	$3D$	4566.37	−8.79	−0.07	+0.23	4557.75	+0.05(20)
	$E2U$	4738.43	−11.91	+0.01	+0.39	4726.92	+1.50(50)
	$3C$	4868.79	−12.81	+0.02	+0.20	4856.20	+1.21(20)
	$3B$	4961.57	−4.84	+0.84	−5.98	4951.60	−2.40(40)
	$3A$	5053.18	−6.09	+0.86	−5.92	5042.03	−2.10(20)
	$E2S$	5193.35	−6.95	+0.86	−6.05	5181.22	−2.45(20)
	$4D$	5923.32	−8.50	−0.03	−0.18	5914.61	+1.66(30)

TABLE IV continued.

Element	*Key*	$E_{Coulomb}$ (eV)	E_{Breit} (eV)	E_{VP} (eV)	E_{SE} (eV)	E_{TOTAL} (eV)	ΔE (eV)
Lanthanum	*M2*	4749.90	−8.17	−0.33	+1.65	4743.04	+1.40(20)
	3G	4755.69	−7.99	−0.33	+1.65	4749.02	+1.34(40)
	E2L	4852.97	−6.63	−0.05	−0.32	4845.98	+1.08(20)
	3D	5146.08	−10.06	−0.04	−0.26	5135.73	+0.62(20)
	3F	5184.21	−14.04	−0.27	+2.17	5172.06	+1.48(20)
	E2U	5398.57	−14.39	+0.02	+0.43	5384.62	+1.69(40)
	3A	5737.04	−7.37	+1.11	−7.29	5723.49	−2.28(40)
	E2S	5891.32	−8.39	+1.11	−7.47	5876.58	−2.78(40)
Neodymium	*M2*	5314.44	−9.59	−0.42	+1.97	5306.39	+1.52(25)
	3G	5320.62	−9.38	−0.42	+1.97	5312.79	+1.38(25)
	3D	5766.89	−11.66	−0.04	−0.45	5754.75	+0.48(40)
	3F	5859.14	−16.99	−0.35	+2.67	5844.46	+2.17(40)
Europium	*M2*	5907.56	−11.15	−0.54	+2.35	5898.22	+1.69(60)
	3G	5914.14	−10.90	−0.54	+2.35	5905.05	+1.80(60)

TABLE V. Theoretical energies of the transitions $3A$, $3B$, and $E2S$. The energies are obtained from optimal level calculations which take into account interactions with states $(2s^2 2p^1 3p3d)_{J=1}$ in the case of transitions $3A$ and $3B$, and interactions with states $(2s^2 2p^1 3d3d)_{J=2}$ in the case of transition $E2S$. E_{CK} is the fraction of E_{TOTAL} which arises from (super) Coster-Kronig fluctuations.

	$3B$		$3A$		$E2S$	
Element	E_{TOTAL} (eV)	E_{CK} (eV)	E_{TOTAL} (eV)	E_{CK} (eV)	E_{TOTAL} (eV)	E_{CK} (eV)
Silver	3597.69	−1.90	3646.28	−1.90		
Xenon	4949.69	−1.91	5040.12	−1.91	5180.32	−0.90
Lanthanum			5721.57	−1.92	5875.68	0.90

Figures

FIG. 1. Minimum central electron temperature necessary to observe x-ray transitions in neonlike ions of atomic number Z with the PLT high-resolution Bragg-crystal spectrometer. The line-averaged electron density in each case was 1×10^{13} cm^{-3}. The solid line is drawn as a visual aid only.

FIG. 2. Overview of the spectra observed in the wavelength range 2.00—3.00 Å showing the location of the x-ray transitions in neonlike xenon, lanthanum, neodymium, and europium with respect to the location of various hydrogen- and heliumlike reference lines. The notation used to label the neonlike transitions is that of Table I. No measurements were made in the interval 2.19—2.29 Å (shaded region).

FIG. 3. Spectrum of the $3s_{1/2} \rightarrow 2p_{3/2}$ transitions, labelled $3G$ and $M2$, in Nd^{50+}. The spectrum was obtained with the PLT high-resolution spectrometer. Also seen are satellites due to $3s_{1/2} \rightarrow 2p_{5/2}$ transitions in lower charge states of neodymium. The data have been accumulated from 33 PLT discharges. The background is due to the bremsstrahlung and recombination continuum.

FIG. 4. Spectrum of the transition $3s_{1/2} \rightarrow 2p_{1/2}$, labelled $3F$, and $3d_{5/2} \rightarrow 2p_{3/2}$, labelled $3D$, in Nd^{50+}. The data have been accumulated from 13 PLT discharges. For elements with $Z \geq 55$ the wavelength of line $3F$ is shorter than the wavelength of line $3D$ as a result of the relativistic splitting of the $2p^5_{3/2}$ and $2p^5_{1/2}$ core levels. The increased line width of line $3D$ compared to line $3F$ is due to a diminished resolution of the spectrometer.

FIG. 5. Comparison of measured and theoretical energies for transitions of the type: (a) $3s_{1/2} \rightarrow 2p_{3/2}$ and $3d, 3p \rightarrow 2s$; (b) $3s_{1/2} \rightarrow 2p_{1/2}$; (c) $3d, 4d \rightarrow 2p$; and (d) $3p \rightarrow 2p$. The theoretical values were calculated in the extended average level approach, except transitions $3C$ and $3D$ which were calculated in the optimum level approach. The solid lines are drawn as a visual aid only.

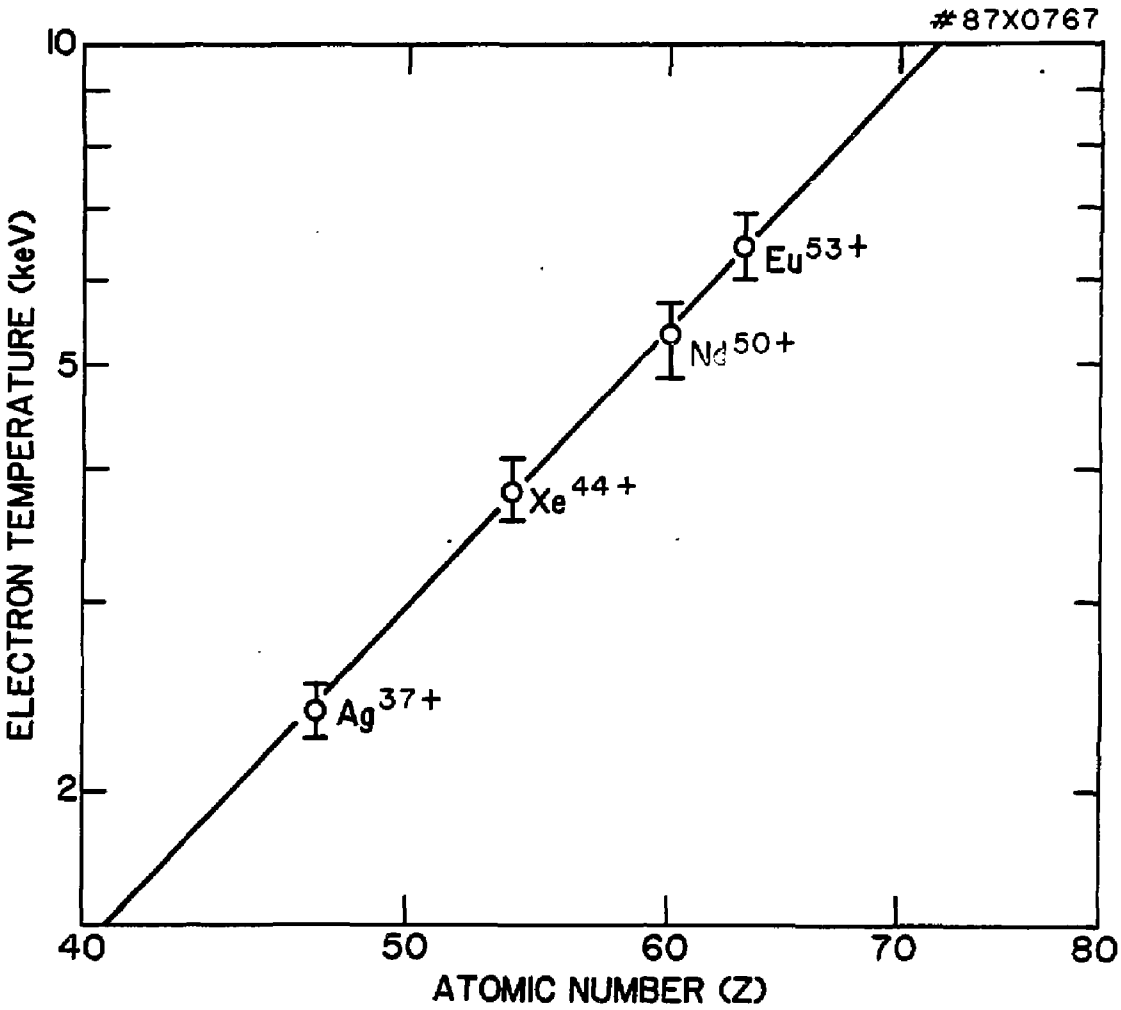
#87X0767
10
5
2
ELECTRON TEMPERATURE (keV)
Ag37+
Xe44+
Nd50+
Eu53+
40
50
60
70
80
ATOMIC NUMBER (Z)

Fig. 1

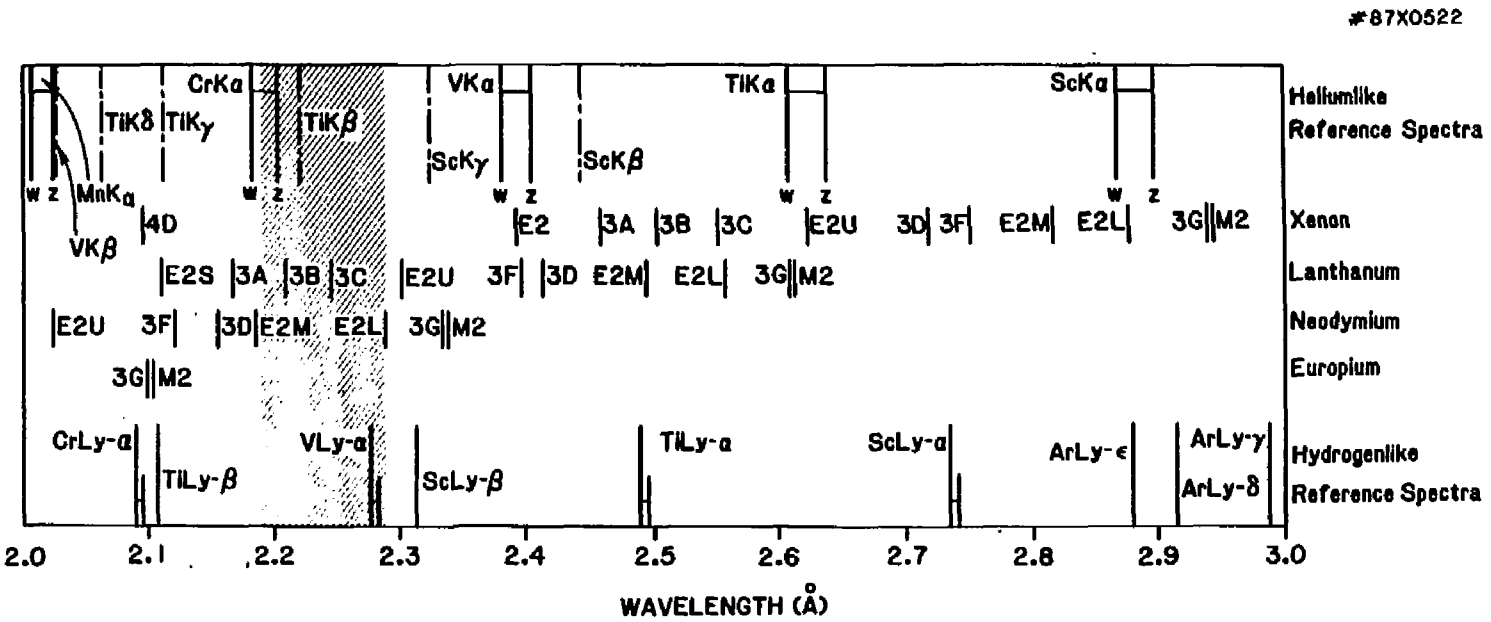
#87X0522
CrKα
TiKδ
TiKγ
TiKβ
VKα
ScKγ
ScKβ
TiKα
ScKα
w z
MnKα
VKβ
4D
E2
3A
3B
3C
E2U
3D
3F
E2M
E2L
3G
M2
E2S
Heliumlike
Reference Spectra
Xenon
Lanthanum
Neodymium
Europium
CrLy-α
TiLy-β
VLy-α
ScLy-β
TiLy-α
ScLy-α
ArLy-ϵ
ArLy-γ
ArLy-δ
Hydrogenlike
Reference Spectra
2.0
2.1
2.2
2.3
2.4
2.5
2.6
2.7
2.8
2.9
3.0
WAVELENGTH (Å)

Fig. 2

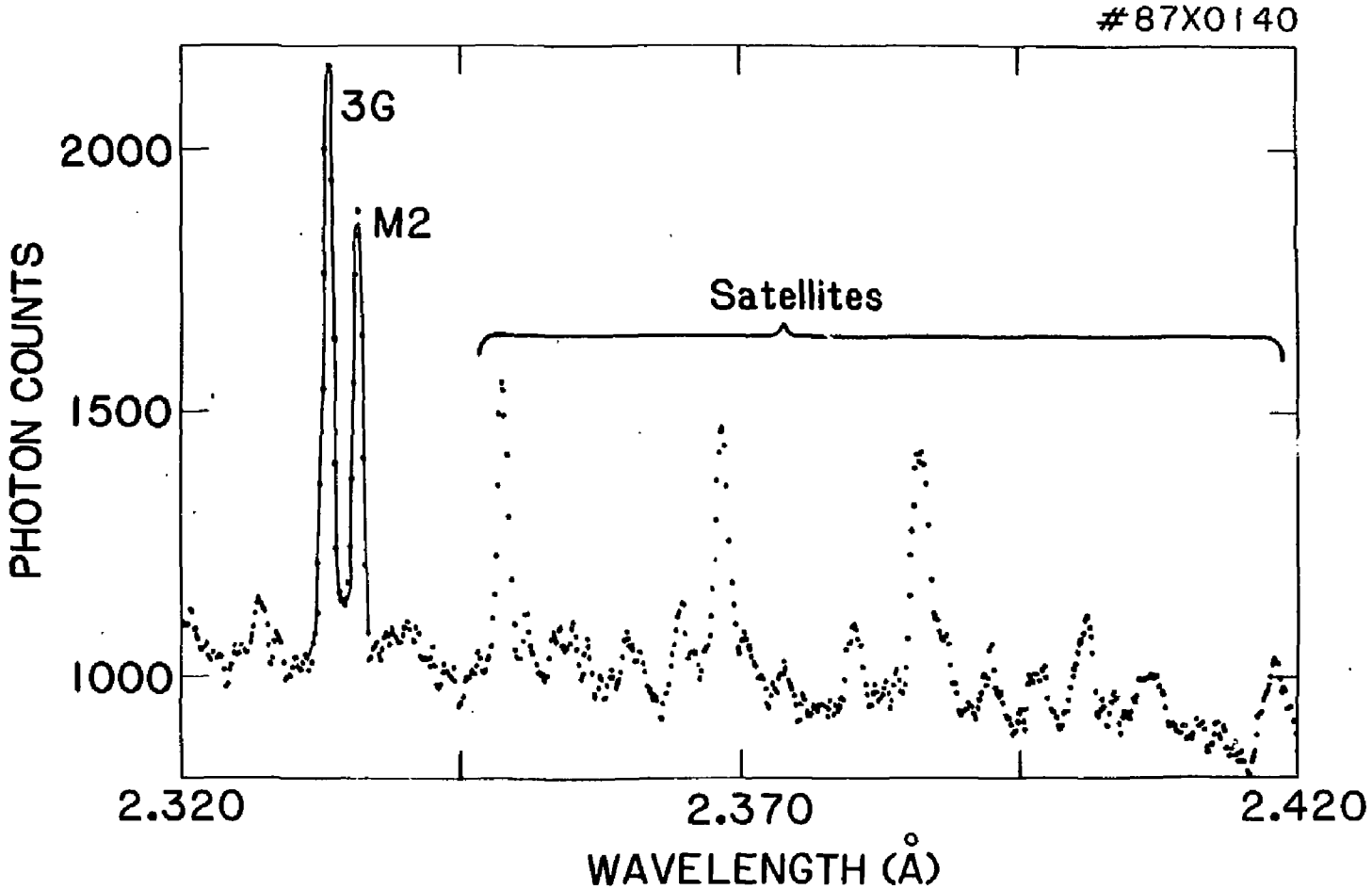
#87X0140
3G
M2
Satellites
2000
1500
1000
PHOTON COUNTS
2.320
2.370
2.420
WAVELENGTH (Å)

Fig. 3

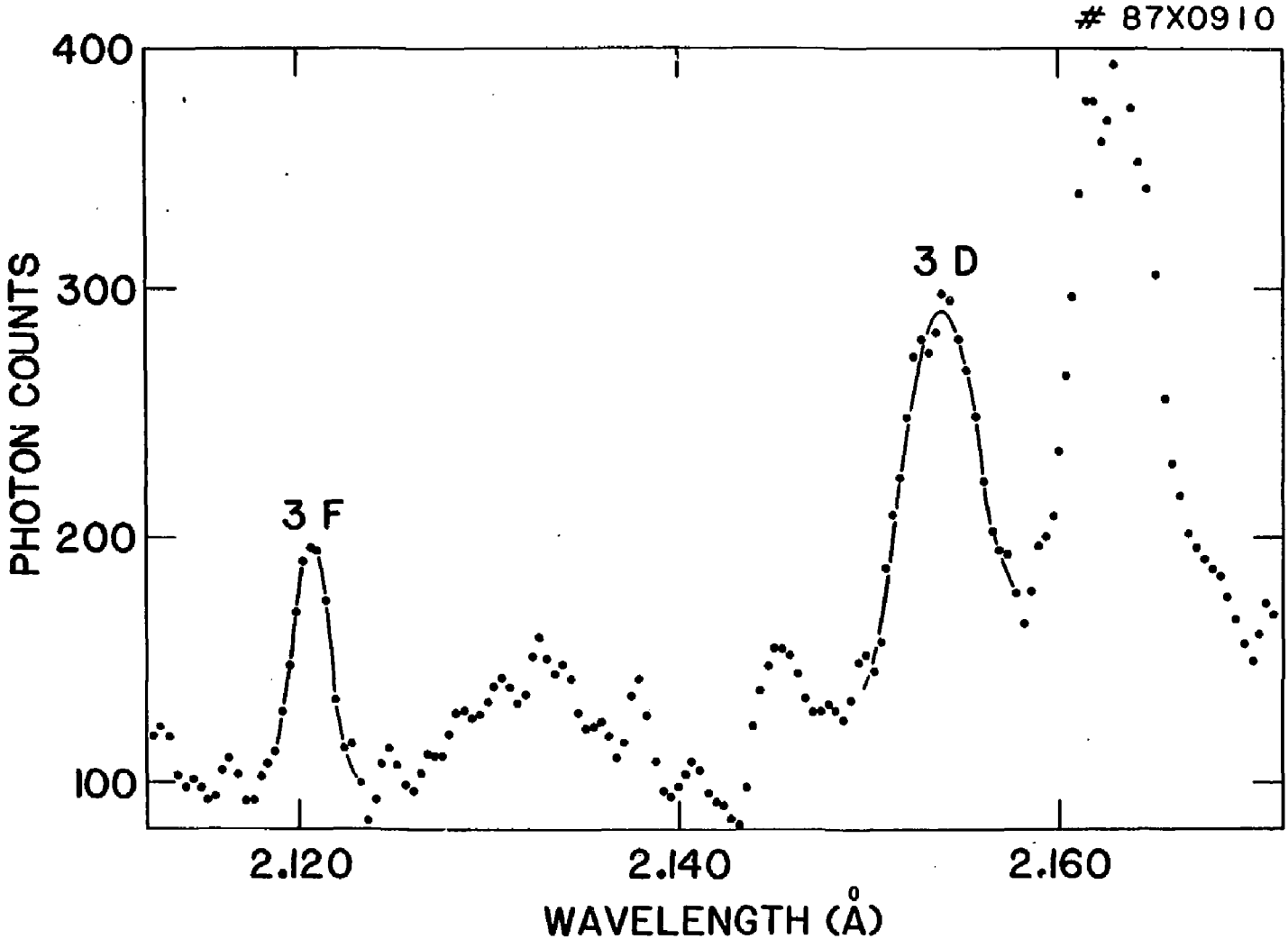
87X0910
400
300
200
100
PHOTON COUNTS
3 F
3 D
2.120
2.140
2.160
WAVELENGTH (Å)

Fig. 4

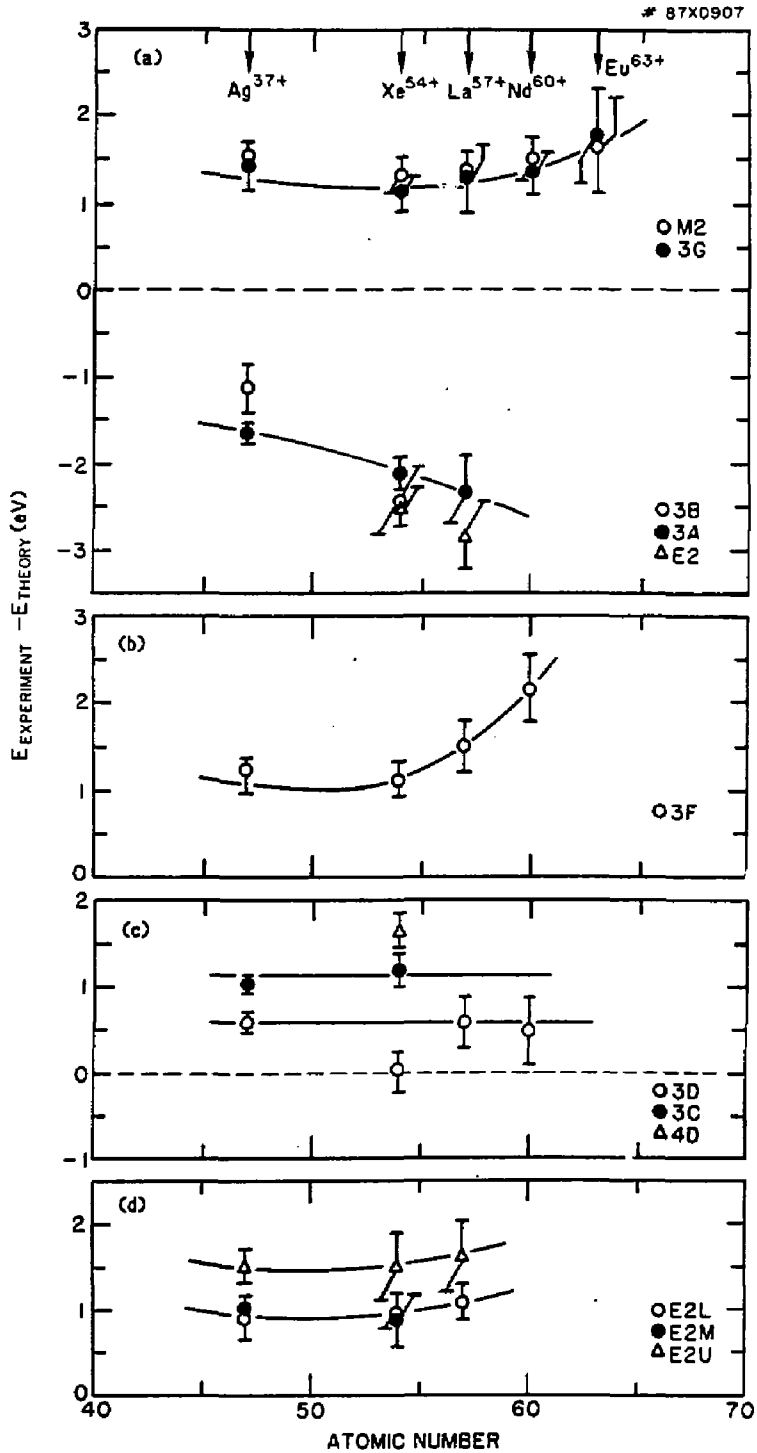
87X0907
(a)
Ag37+
Xe54+
La57+
Nd60+
Eu63+
M2
3G
3B
3A
E2
(b)
3F
(c)
3D
3C
4D
(d)
E2L
E2M
E2U
E EXPERIMENT − E THEORY (eV)
ATOMIC NUMBER

Fig. 5

EXTERNAL DISTRIBUTION IN ADDITION TO UC-20

Dr. Frank J. Paoloni, Univ of Wollongong, AUSTRALIA
Prof. M.H. Brennan, Univ Sydney, AUSTRALIA
Plasma Research Lab., Australian Nat. Univ., AUSTRALIA
Prof. I.R. Jones, Flinders Univ., AUSTRALIA
Prof. F. Cap, Inst Theo Phys, AUSTRIA
Prof. M. Heindler, Institut fur Theoretische Physik, AUSTRIA
M. Goossens, Astronomisch Instituut, BELGIUM
Ecole Royale Militaire, Lab de Phys Plasmas, BELGIUM
Commission-European, Dg-XII Fusion Prog, BELGIUM
Prof. R. Boucique, Laboratorium voor Natuurkunde, BELGIUM
Dr. P.H. Sakanaka, Instituto Fisica, BRAZIL
Instituto De Pesquisas Espaciasi-INPE, BRAZIL
Documents Office, Atomic Energy of Canada Limited, CANADA
Dr. M.P. Bachynski, MPB Technologies, Inc., CANADA
Dr. H.M. Skarsgard, University of Saskatchewan, CANADA
Dr. H. Barnard, University of British Columbia, CANADA
Prof. J. Teichmann, Univ. of Montreal, CANADA
Prof. S.R. Sreenivasan, University of Calgary, CANADA
Prof. Tudor W. Johnston, INRS-Energie, CANADA
Dr. C.R. James, Univ. of Alberta, CANADA
Dr. Peter Lukac, Komenskeho Univ, CZECHOSLOVAKIA
The Librarian, Culham Laboratory, ENGLAND
The Librarian, Rutherford Appleton Laboratory, ENGLAND
Mrs. S.A. Hutchinson, JET Library, ENGLAND
C. Mouttet, Lab. de Physique des Milieux Ionises, FRANCE
J. Radet, CEN/CADARACHE - Bat 506, FRANCE
Univ. of Ioannina, Library of Physics Dept. GREECE
Dr. Tom Mual, Academy Bibliographic Ser., HONG KONG
Preprint Library, Hungarian Academy of Sciences, HUNGARY
Dr. B. Dasgupta, Saha Inst of Nucl. Phys., INDIA
Dr. P. Kaw, Institute for Plasma Research, INDIA
Dr. Philip Rosenau, Israel Inst. Tech, ISRAEL
Librarian, Int'l Ctr Theo Phys, ITALY
Prof. G. Rostagni, Univ Di Padova, ITALY
Miss Clelia De Palo, Assoc EURATOM-ENEA, ITALY
Biblioteca, Instituto di Fisica del Plasma, ITALY
Dr. H. Yamato, Toshiba Res & Dev, JAPAN
Prof. I. Kawakami, Atomic Energy Res. Institute, JAPAN
Prof. Kyoji Nishikawa, Univ of Hiroshima, JAPAN
Direc. Dept. Large Tokamak Res. JAERI, JAPAN
Prof. Satoshi Itoh, Kyushu University, JAPAN
Research Info Center, Nagoya University, JAPAN
Prof. S. Tanaka, Kyoto University, JAPAN
Library, Kyoto University, JAPAN
Prof. Nobuyuki Inoue, University of Tokyo, JAPAN
S. Mori, JAERI, JAPAN
Librarian, Korea Advanced Energy Res. Institute, KOREA
Prof. D.I. Choi, Adv. Inst Sci & Tech, KOREA
Prof. B.S. Liley, University of Waikato, NEW ZEALAND
Institute of Plasma Physics, PEOPLE'S REPUBLIC OF CHINA
Librarian, Institute of Phys., PEOPLE'S REPUBLIC OF CHINA
Library, Tsing Hua University, PEOPLE'S REPUBLIC OF CHINA
Z. Li, Southwest Inst. Physics, PEOPLE'S REPUBLIC OF CHINA
Prof. J.A.C. Cabral, Inst Superior Tecnico, PORTUGAL
Dr. Octavian Petrus, AL I CUZA University, ROMANIA
Dr. Johan de Villiers, Fusion Studies, AEC, SO AFRICA
Prof. M.A. Hellberg, University of Natal, SO AFRICA
C.I.E.M.A.T., Fusion Div. Library, SPAIN
Dr. Lennart Stenflo, University of UMEA, SWEDEN
Library, Royal Inst Tech, SWEDEN
Prof. Hans Wilhelmson, Chalmers Univ Tech, SWEDEN
Centre Phys des Plasmas, Ecole Polytech Fed, SWITZERLAND
Bibliotheek, Fom-Inst Voor Plasma-Fysica, THE NETHERLANDS
Dr. D.D. Ryutov, Siberian Acad Sci, USSR
Dr. G.A. Eliseev, Kurchatov Institute, USSR
Dr. V.A. Glukhikh, Inst Electrophysical Apparatus, USSR
Dr. V.T. Tolok, Inst. Phys. Tech. USSR
Dr. L.M. Kovrizhnykh, Institute Gen. Physics, USSR
Nuclear Res. Establishment, Julich Ltd., W. GERMANY
Bibliothek, Inst. Fur Plasmaforschung, W. GERMANY
Dr. K. Schindler, Ruhr Universitat Bochum, W. GERMANY
ASDEX Reading Rm, IPP/Max-Planck-Institut fur Plasmaphysik, W. GERMANY
Librarian, Max-Planck Institut, W. GERMANY
Prof. R.K. Janev, Inst Phys, YUGOSLAVIA